

Effects of Alkali Treatment on the Microstructure, Composition, and Properties of the *Raffia textilis* Fiber

Raymond Gentil Elenga,^{a,*} Philippe Djemia,^b David Tingaud,^b Thierry Chauveau,^b Jean Goma Maniongui,^a and Guy Dirras^b

The *Raffia textilis* fiber has a specific strength of 660 MPa·cm³/g and scales and hollows on its surface. Thus, this fiber is a potential composite reinforcement. The objective of this study was to evaluate the effect of alkaline treatment at room temperature on its microstructure, structure, composition, thermal behavior, mechanical properties, and color. To this end, slack raw fibers were soaked in three NaOH solutions (2.5%, 5%, and 10% by weight) for 12 hours. SEM observations revealed that fibers got more and more clean and smooth when the solution concentration was increased. In comparison with the raw fiber, it was found that fiber treated with 5% NaOH solution exhibited enhanced tensile strength (129%) and strain to failure (175%), in addition to increased yellowness, redness, and thermal stability. Contrariwise, the Young modulus and lightness slightly decreased with the treatment. The Fourier transform infrared spectra and the XRD patterns suggested an incipient allotropic transformation of cellulose for 10% NaOH-treated fibers. These changes could be explained by the gradual dissolution of non-cellulosic components as revealed by the Fourier transform infrared attenuated total reflection spectra and thermal analysis.

Keywords: Natural fiber; *Raffia*; Alkali treatment; Thermal degradation; Mechanical properties; Microstructure; Crystal structure; Cellulose; Color

Contact information: a: Laboratoire des Matériaux et Energies, Faculté des Sciences, Université Marien N'Gouabi; b: Université Paris 13, Sorbonne Paris Cité, LSPM-CNRS, 99 av. Jean-Baptiste Clément, 93430 Villetaneuse, France; *Corresponding author: rgelenga@gmail.com

INTRODUCTION

The necessity of preserving the environment and increasing the use of renewable natural resources has led to the use of natural fibers in several industrial sectors, including polymer composites, building materials, technical textiles, and geotextiles (Bledzki and Gassan 1999; John and Thomas 2008). It is expected that newly passed legislation, in the EU for instance, will increase their demand even further (Jawaid and Abdul Khalil 2011; John and Thomas 2008). The rising demand has increased the use of plant fibers that have previously been neglected such as coir, bamboo, curaua, bagasse, and pineapple (Jawaid and Abdul Khalil 2011; Satyanarayana *et al.* 2007). Many of these new fibers are grown in tropical areas, and their industrial use should contribute to improving the living conditions in these areas. However, the expansion of agriculture is currently considered the greatest threat to biodiversity, including primary forests (Koh *et al.* 2010; Tilman *et al.* 2001). Thus, the sustainable exploitation of endemic wildlife-friendly fiber plants is a compromise between the duty to preserve biodiversity and the necessity of fighting poverty. From this perspective, multifunctional plants, or the ones that can be harvested several times in a growing cycle, are the most interesting.

The raffia palm tree belongs to the above-mentioned multifunctional plants category. Many of its parts have well known uses such as textiles, medicine, carpet, broom, palm wine, raffia oil, and building material (Edem *et al.* 1984, 2009). The raffia fiber resembles a strap and is actually the leaflet epidermis of a young leaf. A recent investigation reported its microstructure and some interesting properties, such as its average specific strength of about 660 MPa-cm³/g (Elenga *et al.* 2009), which is comparable to other natural fibers and synthetic fibers, such as E-glass, that are being used as composite reinforcements (Bledzki and Gassan 1999; Monteiro *et al.* 2011). Its microstructure exhibits alveoli on the bottom face and usually scales on the top one. These features could facilitate mechanical anchoring with a polymer matrix. Therefore, this fiber has interesting potential as composite reinforcement.

In the context of composite processing, it is also important to know the thermal behavior of the fiber. Although plant fibers have almost the same major components (cellulose, hemicellulose, lignin, and pectin), their thermal behavior varies from one fiber to another (D' Almeida *et al.* 2008; Yao *et al.* 2008). Indeed, this behavior depends on the proportion of these components and on the cellulose structure. To enhance the fiber-matrix adhesion and the fiber's mechanical properties, various physical and chemical treatments are applied (Bledzki and Gassan 1999; George *et al.* 2001). Among them, treatment with sodium hydroxide is typical and cheap. Previous studies on this type of treatment have revealed that its effects depend mainly on the fiber type, the NaOH concentration, and the soaking temperature and duration (Bledzki and Gassan 1999; Saha *et al.* 2010; Van de Weyenberg *et al.* 2006). For instance, Saha *et al.* (2010) reported that the tensile strength of jute fiber increased continuously with the concentration between 0% and 4% NaOH. However, the maximum tensile strength was reached after 4 h of soaking in 0.5% NaOH and 30 min in 4% NaOH solution. On the contrary, the maximum tensile strength of coir fiber soaked in 5% NaOH solution was reached after 70 h of soaking (Bledzki *et al.* 1999). To our knowledge, the alkalization of raffia fiber has not yet been studied. However, such studies have been performed on fibers from other palm trees species. AlMaadeed *et al.* (2013) reported that after 2 h soaking at 100 °C, the tensile strength of the leaflet fibers of female date palm decreased continuously with the increase of the NaOH concentration. Contrariwise, for leaflet fibers of male date palm, the tensile strength varied parabolically, and the maximum value was obtained for fibers treated in 2% NaOH. In comparison with raw fibers, the tensile strength increase of treated fibers was about 33%. For fibers that surround the date palm trunk, Alawar *et al.* (2009) reported that after 1 h soaking at 100 °C, the tensile strength was maximal for 1% treated fibers. The increase was about 400% compared to the raw fiber. On the contrary, the Young's modulus decreased continuously with the increase of the concentration. At room temperature, for the same fibers, Alsaeed *et al.* (2013) showed that for 24 h soaking in solution with concentration between 3 to 9%, the tensile strength decreased. For oil palm empty fruit bunches fibers (OPEFBF), according to Norul Izani *et al.* (2013), treatment at room temperature in 2% NaOH solution improved the strength and the Young's modulus by 23% and 9%, respectively.

In previous studies, the mechanical and physical properties of the raw *Raffia textilis* fiber were characterized (Elenga *et al.* 2009), and its drying kinetics were modeled (Elenga *et al.* 2011). The objective of the present study is to investigate the effect of sodium hydroxide treatment on the microstructure, structure, composition, thermal behavior, mechanical properties, and color of the *Raffia textilis* fiber.

EXPERIMENTAL

Fibers Preparation

The raw fibers were extracted from young leaves of wild *Raffia textilis* palm trees. The extraction process was performed by removing the upper epidermis of the leaflet with a knife. This procedure was carried out, at most, 48 h after harvest. After the extraction, the fibers were dried in air at room temperature (RT, about 25 °C) until their mass reached equilibrium. The mean value of the moisture content of dried fiber was 17% by weight, on a dry basis. The obtained fibers had dimensions of about 0.5 cm wide, 30 to 40 cm long, and 15 μm thick. Their color was light yellow.

For the sodium hydroxide treatments (NaOH) of fibers, three NaOH concentrations were prepared (2.5%, 5%, and 10% by weight) by dissolving sodium hydroxide pellets (98% purity) in distilled water. These concentrations were chosen to preserve the cellulose part of the fiber. Dried and slack raw fibers were completely soaked in the NaOH solutions for 12 h at RT. After immersion, the treated fibers were washed in running tap water, followed by distilled water until the wash water became neutral (pH = 7). They were then dried again at RT.

Scanning Electron Microscopy

To investigate the microstructure and the surface morphology of raw and treated fibers, samples having a surface area of about 0.5 cm² were cut off and coated with 5 nm of carbon for scanning electron microscope (SEM) studies using a Zeiss Supra 40VP FEG SEM instrument. These investigations were performed on both the top and bottom faces of the fiber.

Infrared Spectra Measurements

The Fourier transform infrared attenuated total reflexion (FTIR-ATR) spectra were recorded on a Perkin Elmer GX spectrometer with an accessory diamond ATR. One hundred acquisitions were performed in the range 400 to 4000 cm⁻¹. As suggested by Oh *et al.* (2005), the band at 894 cm⁻¹ was used as the internal standard band to determine the crystallinity index (CI) and the band intensity ratios. Indeed, these authors reported that the CI calculated with this band as an internal standard has the best correlation coefficient with the CI determined by X-ray diffraction (XRD).

X-ray Scattering Analysis

X-ray diffraction (XRD) experiments were performed on an automated InelTM four-circle goniometer. The monochromatic beam of wavelength 1.5405 Å (CuKα1) was obtained after reflection on the {111} planes of germanium single crystal and the elimination of Kα2 radiation. Given its low degree of crystallinity, the fibers were folded several times before being fixed on the sample holder. The X-ray diffractograms were recorded from 5.5 to 100° in 2θ mode by a curved linear detector (Inel CPS 590) with an angular resolution of 0.015°.

In a first approximation and neglecting the lattice distortion, the apparent crystallite size was calculated through use of Scherer's formula.

$$L = \frac{K\lambda}{B \cos \theta} \quad (1)$$

In Eq. 1, $K = 0.89$ is the Scherrer constant, θ is the diffraction angle, B is the full-width in radians at the half-height of the peak, and λ is the X-ray wavelength (Hindeleh and Johnson 1980).

The crystallinity index (CI) was estimated by using the Segal formula (Bansal *et al.* 2010),

$$CI = \frac{H_{22.5} - H_{18.5}}{H_{22.5}} \quad (2)$$

where $H_{22.5}$ and $H_{18.5}$ are diffractogram intensities at 22.5 and 18.5° , attributed to (002) plane and amorphous part, respectively.

Thermal Degradation

For all types of fibers, thermal degradation was investigated by the measurement of the fiber mass loss from 40 to 600°C at a heating rate of $10^\circ\text{C}/\text{min}$. The flowing gas was air, which was selected in order to provide conditions conducive to degradation. These measurements were carried out in a TAG 24 Setaram apparatus. To improve the heat-mass transfer, small pieces of a fiber were cut out and plated against the crucible bottom and the sample weight was limited to 2.5 mg because its density was about 0.75 g/cm^3 . Thus, its thickness was less than 2 mm in the crucible.

Tensile Tests

The tensile tests were performed by the use of an Instron mono-column universal testing machine model 5544, with a load capacity of 2 kN and a sensitivity on the order of 0.5% . To avoid breaking the sample within the grips, the fiber was mounted by affixing the extremities of the fiber on a piece of balsa or cardboard, which was then pinched in the grips. The sample had a mean cross section of 0.015 mm \times 5 mm and an initial gauge length of 60 mm. The strain rate was about 3×10^{-4} s^{-1} . For each treatment, at least 16 replicas of the test were carried out.

Color Measurements

Color measures were performed using a Minolta spectrophotometer, 3200d model, with three illuminants (D65, A, and F2). The fiber color was expressed by the L^* , a^* , and b^* coordinates of the *Commission Internationale d'Eclairage* color space. The values of L^* , a^* , and b^* represent darkness-lightness, greenness-redness, and blueness-yellowness, respectively. L^* varies from 100 for perfect white to zero for black, a^* measures redness when positive, gray when zero, and greenness when negative, and b^* measures yellowness when positive, gray when zero, and blueness when negative. Thus, an increase of L^* , a^* , and b^* denotes more white, red chroma, and yellow chroma, respectively. The variation of color (ΔE) was estimated in comparison to the raw fiber by the formula,

$$\Delta E^* = [(L^* - L_r^*)^2 + (a^* - a_r^*)^2 + (b^* - b_r^*)^2]^{1/2} \quad (3)$$

where the coordinates without a subscript are those of the treated fiber and those with the subscript (r) are those of the raw fiber.

RESULTS AND DISCUSSION

Microstructure

SEM micrographs of fibers treated at different NaOH concentrations are shown in Fig. 1. The main observation was that the fibers were more and more clean and smooth with increasing solution concentration. It was also observed that the alveoli (bottom face) were more sensitive to NaOH concentration than the top face. For instance, after 10% NaOH treatment of fibers, the alveoli almost disappeared and the fibrils were less tied together. As it will be shown by ATR-FTIR analysis described in the next section, alkaline treatments dissolve mainly hemicellulose and lignin. Therefore, it can be concluded that they are probably the major constituents of alveoli. Additionally, the top faces observed here did not have scales, contrary to those reported in a previous report (Elena *et al.* 2009).

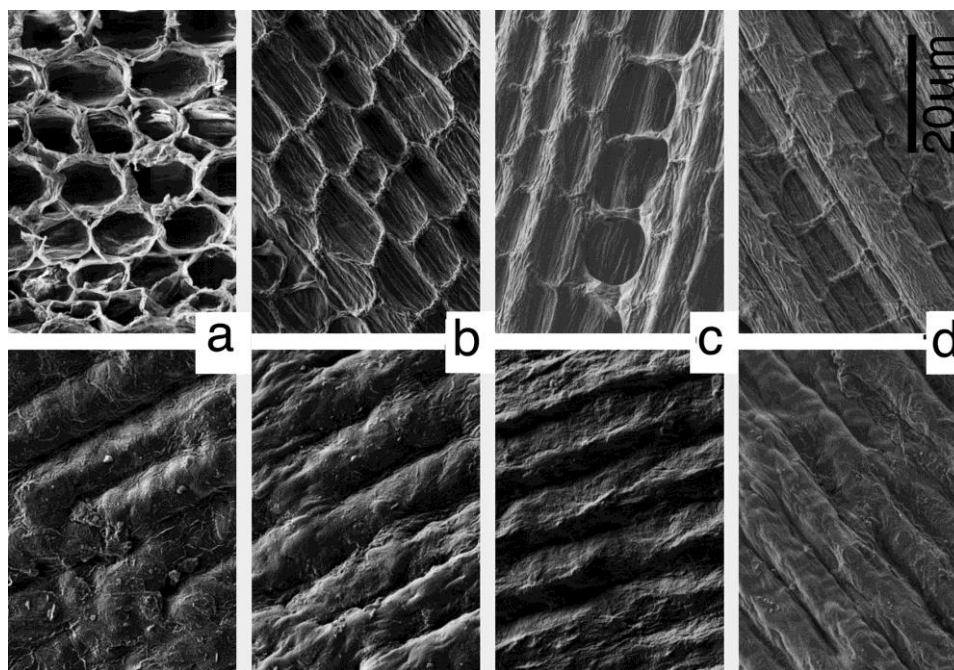


Fig. 1. Micrographs of the bottom (honeycomb, first line) and top faces of raffia fibers (second line); from left to right: untreated (a), treated with 2.5% (b), 5% (c), and 10% NaOH concentrations, respectively

FTIR Analysis

The FTIR-ATR spectra of the raw and NaOH-treated fibers showed characteristic bands that can be assigned to components of lignocellulosic fibers (LCFs) as shown in Fig. 2a and 2b. As can be seen in these diagrams, the signal intensity increased with the solution concentration. This effect is consistent with the evolution of the fiber's surface with the treatments shown by the SEM micrographs. Cleanliness and smoothness of the fiber increased with the solution concentration. Due to this effect and to the inherent

variability of LCFs characteristics (compared to synthetic fibers), the comparison between the spectra will be based on the relative intensity of the peaks, taking as reference the band at 897 cm^{-1} (here at 894 cm^{-1}) proposed by Oh *et al.* (2005).

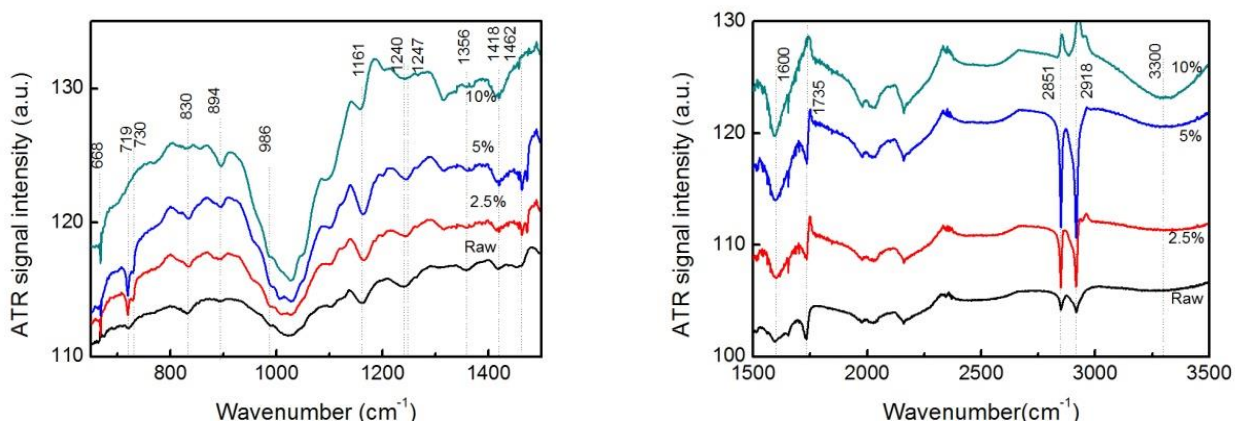


Fig. 2. FTIR-ATR spectra of raw and NaOH-treated fibers; peaks of the major components of the fiber are shown: cellulose I_{β} (719 cm^{-1}), lignin (830 , 1240 , and 1462 cm^{-1}), and hemicellulose (1161 , 1247 , and 1735 cm^{-1})

The band at 668 cm^{-1} is attributed to the celluloses I and II (Kondo and Sawatari 1996). Its intensity increased with the NaOH concentration without the peak shifting. Oh *et al.* (2005) reported this band's behavior during the conversion of cellulose I to cellulose II by alkali treatment.

The absorbance at 719 cm^{-1} was attributed to the cellulose I_{β} (Sugiyama *et al.* 1991). The absorbance ratio between this band and the standard band at 894 cm^{-1} has been reported as having the highest correlation with the XRD CI (Oh *et al.* 2005). Thus, it could be considered as a measure of CI. With a NaOH concentration of up to 5%, the CI did not vary significantly, as shown in Fig. 3. However, for the 10% NaOH-treated fibers, the observed CI decrease was about 60%.

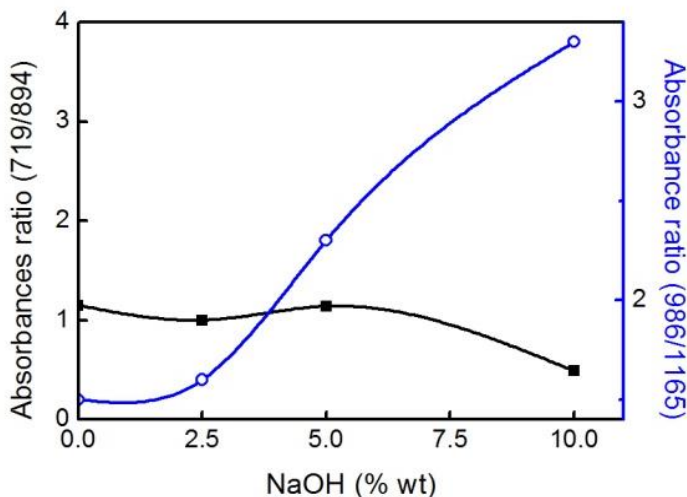


Fig. 3. Effect of NaOH concentration on the peaks assigned to cellulose I_{β} (719 and 1165 cm^{-1}) and cellulose II (986 cm^{-1})

The decrease of the CI linked to the cellulose I_{β} is consistent with the transformation of cellulose I to the cellulose II suggested by the increase of the band at 668 cm^{-1} . In addition, this band and the band at 1430 cm^{-1} , which was also assigned to the crystalline structure, were broader for fiber treated with 10% NaOH than the raw fiber. This could reflect a more disordered structure of the treated fiber. For 2.5% and 5% NaOH solutions, a new band appeared at 730 cm^{-1} , which, to our knowledge, has never been reported for lignocellulosic fibers. Further investigation is probably needed to clarify this point. Oh *et al.* (2005) reported that the absorbance at $983\text{--}993\text{ cm}^{-1}$ increased, whereas the band at 1165 cm^{-1} decreased during cellulose transformation. Therefore, the corresponding ratio (986/1161) would increase during this transformation, which is in line with the experimental results shown in Fig. 3.

The absorbances at 830 , 1240 , and 1462 cm^{-1} were attributed to lignin, whereas those at 1161 , 1247 , and 1735 cm^{-1} were attributed to hemicelluloses (Sun *et al.* 1996; Zuluaga *et al.* 2009). Figure 4 shows the ratios of four of these bands with the standard band at 894 cm^{-1} versus NaOH concentration. All these ratios were weaker for treated fibers than those of raw fiber, and the ratios of the 10% NaOH-treated fiber were the weakest. Moreover, the lignin peaks and the hemicellulose peak at 1161 cm^{-1} (also attributed to cellulose) and that at 1247 cm^{-1} , which overlapped with that of lignin (1240 cm^{-1}), were reduced less than the hemicellulose peak at 1735 cm^{-1} (also attributed to pectin) (Bociek and Welti 1975). This indicates, as already reported for hemp (Kostic *et al.* 2008), that alkali treatments actually remove more hemicellulose than lignin. The band at 1356 cm^{-1} was attributed to the OH group in cellulose. Its intensity was weaker for alkali-treated fiber. This decrease could be explained by the following reaction (George *et al.* 2001):

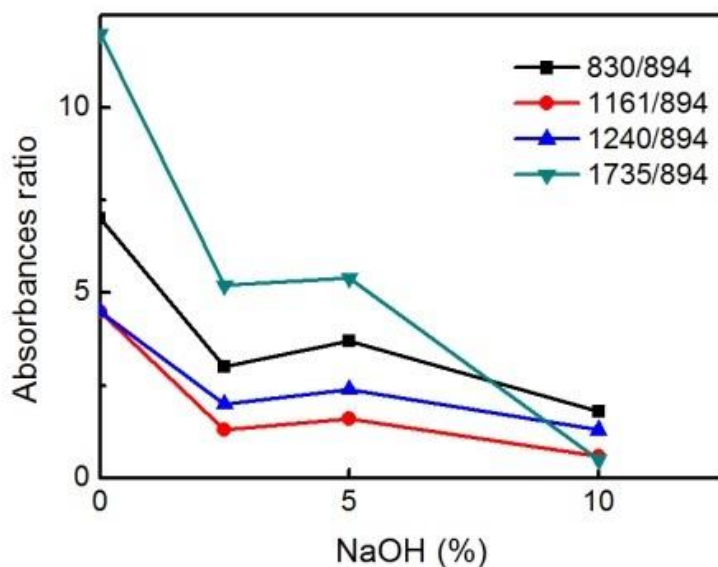


Fig. 4. Evolution of hemicellulose and lignin bands as a function of NaOH concentration. Band intensities decrease when concentration increases.

The peak around 1600 cm^{-1} , which is related to adsorbed water (Yan *et al.* 2009; Zafeiropoulos *et al.* 2003), increased steadily with NaOH concentration. This result is consistent with the thermal analysis (Fig. 6): treated fibers contained more water than the raw ones (peaks around $80\text{ }^{\circ}\text{C}$). The broad band around 3300 cm^{-1} was assigned to OH groups and hydrogen bonds of different origins (Oh *et al.* 2005).

The bands at 2851 and 2918 cm^{-1} were assigned to wax, cutin, and chlorophyll (Chapados 1985; Yan *et al.* 2009), but they are also affected by the oxygen/carbon ratio (Zafeiropoulos *et al.* 2003). These bands were strongly reduced only for the fiber treated with 10% NaOH solution.

X-ray Scattering of the Fibers

The X-ray patterns of the fibers are reported in Fig. 5. Taking into account both the overlapping of the peaks (110), (10 $\bar{1}$), and (021) and the weakness of the peaks (130) and (040), the crystallite sizes were calculated from only the peak (002). These values, along with those of the crystallinity index, are reported in Table 1. For the raw and all treated fibers, the peaks exhibited are those of the native monoclinic crystal cellulose I $_{\beta}$ (Fink *et al.* 1995; Jiang *et al.* 2012; Sugiyama *et al.* 1991; Zugenmaier 2001). However, as it can be seen in Fig. 5 or from the evolution of the crystallite size reported in Table 1, the diffractogram shape varied significantly with NaOH concentration.

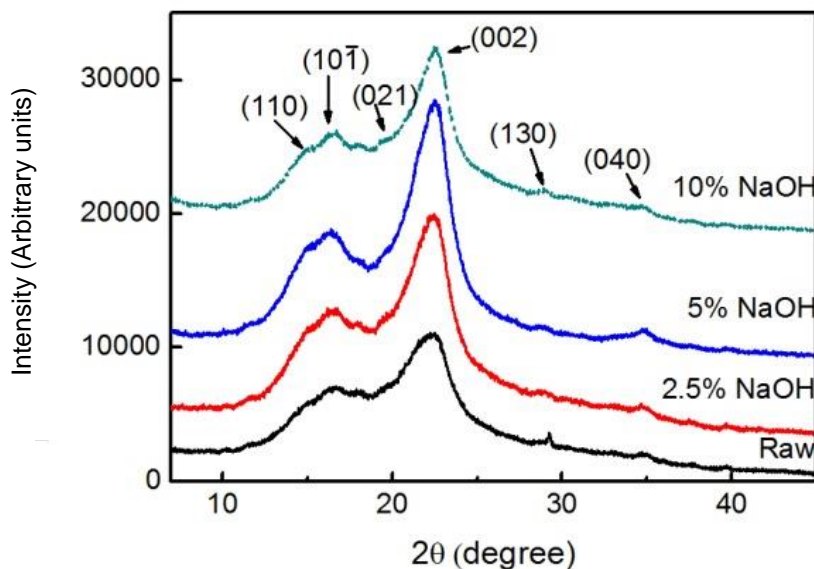


Fig. 5. X-ray diffractograms of raffia fiber as a function of NaOH treatment. The observed peaks could be attributed to cellulose I $_{\beta}$.

Peak broadening depends principally on the crystallite size (Fink *et al.* 1995). For all treated fibers, the crystallite size and the crystallinity index were higher than those of the raw fiber. The highest values were obtained with the 5% NaOH-treated fibers. Compared to the raw fiber, the increase of crystallite size and crystallinity index of the 5% NaOH-treated fibers were 36% and 33%, respectively. These trends were also observed with other fibers. The dissolution of hemicellulose and lignin that separate parallel crystallites enabled some of them to join, mainly by intermolecular hydrogen bonding (Jiang *et al.* 2012). The removal of hemicellulose and lignin, which are

amorphous components of the fiber, also contributes to the increase of the crystallinity index.

For higher NaOH concentrations, Na⁺ ions penetrate and swell crystallites (Van de Weyenberg *et al.* 2006; Satyanarayana *et al.* 2007). This swelling may dissolve less ordered crystallites and may explain the decrease of the crystallinity index for 10% NaOH-treated fibers. The swelling of the crystallites is the beginning of the polymorphic transformation of cellulose I_β to cellulose II.

Thermal Analysis

The TGA and DTG curves of the raw and treated fibers are reported in Fig. 6a and 6b. The main peaks of the thermal decomposition of the raw fiber varied significantly with treatment. The first peak around 80 °C is due to the evaporation of absorbed water and it corresponds to a mass loss of about 5%. It should be noted that the fiber treated with 10% NaOH solution, for which the FTIR spectrum does not present wax peaks, has more absorbed water, as revealed by the increase of the FTIR peak around 1600 cm⁻¹.

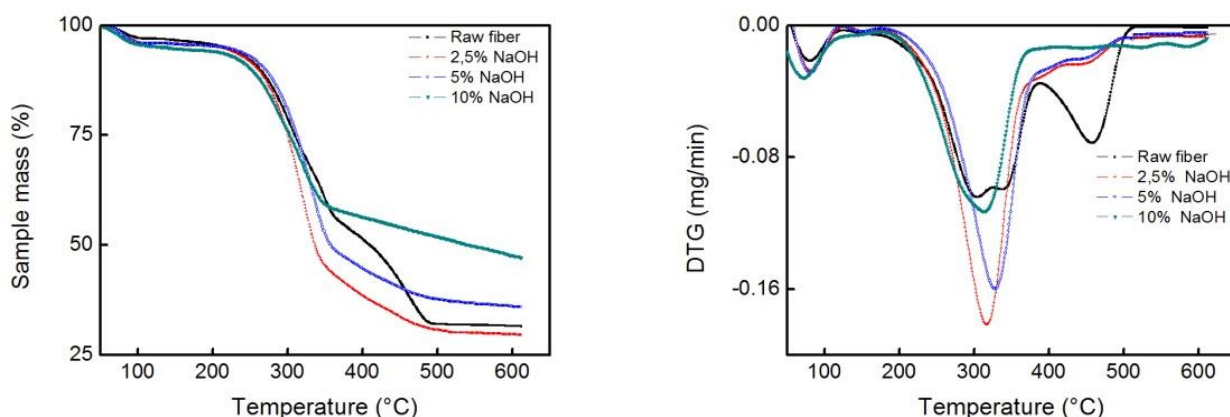


Fig. 6. Evolution of the fiber mass and of its derivative during fiber heating at a rate of 10 °/min in air. The peaks in DTG are related to the decomposition of absorbed water (80 °C), hemicellulose (303 °C), cellulose (340 °C), and lignin (460 °C).

The raw fiber exhibited two overlapping peaks at 303 and 340 °C. According to the thermal analysis of hemicellulose, cellulose, lignin, and other LCFs reported in the literature (D' Almeida *et al.* 2008; Yao *et al.* 2008), the first peak could be attributed to hemicellulose and pectin degradation, while the second one may be due to cellulose decomposition. It has been reported that piassava fiber and oil palm fiber (piassava is another palm tree species), also exhibit two peaks in this temperature range, more precisely, at 303.6 and 377 °C for piassava fiber (D' Almeida *et al.* 2008) and 306 and 365 °C for oil palm fiber (Luangkiattikhun *et al.* 2008). For treated fibers, there was only one peak within the aforementioned temperature range. This fact could be explained by the removal of hemicellulose and pectin by alkali treatment, in accordance with FTIR-ATR analysis.

The last peak at about 460 °C decreased significantly with alkali treatment and disappeared for fiber treated with 10% NaOH solution, which could be attributed to lignin decomposition. This result is in line with the decrease of the lignin FTIR-ATR peaks observed for treated fibers as shown by Fig. 2a and 2b.

The thermal degradation onsets of the raw, 2.5%, 5%, and 10% NaOH-treated fibers were 256 °C, 272 °C, 278 °C, and 250 °C, respectively. This variation of the

thermal degradation onset with the concentration could be explained by: (i) the removal of hemicellulose, which is the least stable of the three major constituents of the fiber and (ii) the destabilization of the native cellulose in 10% NaOH solution. The onset of the raw raffia fiber (256 °C) is higher than the average value reported for plant fibers (219 °C) (Yao *et al.* 2008).

On average, there are more residues created by the treated fibers than for raw fiber. A more detailed explanation of these variations requires analysis of these residues and gases emitted during heating.

Mechanical Behavior

Figure 7 shows typical examples of the stress-strain curves of untreated and treated fibers. In a previous work on the raw *Raffia textilis* fiber (Elenga *et al.* 2009), the stress-strain curve after tensile testing at RT exhibited the typical behavior of a semi-crystalline polymer below the glass transition temperature. At a strain of about 0.7%, the fiber yielded and then deformed by shear band propagation at nearly constant stress until failure. The behavior of the samples investigated here strongly departed from that in the above-mentioned report. The macroscopic behavior of the investigated fiber was characterized by brittle failure. In addition, the examination of the surface of the fractured fibers (not shown) showed that the samples did not break all at once, but rather in stages, involving tearing of the fibers. This behavior is consistent with the reduction of links between fibrils that was observed under SEM.

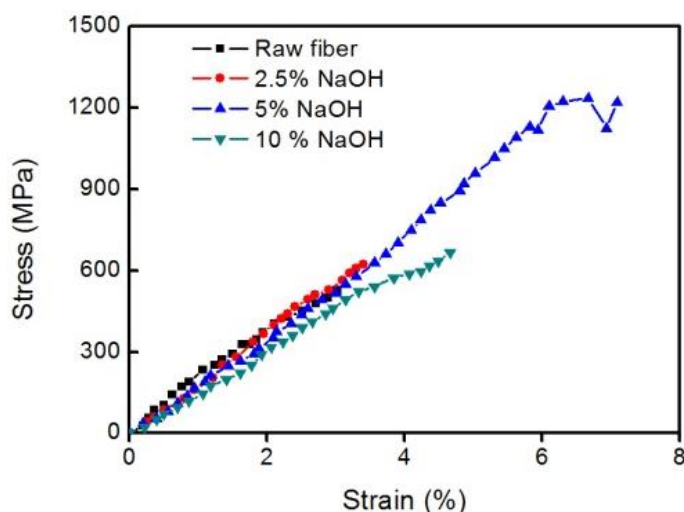


Fig. 7. Stress-strain curves following RT tensile tests ($3.2 \times 10^{-3} \text{ s}^{-1}$) of the raw and NaOH-treated fibers

The effects of alkaline treatment on tensile strength, Young's modulus, and elongation at failure are summarized in Table 1. Each value presented is an average of at least sixteen tests. It can be observed that while the Young's modulus slightly decreased with increasing NaOH concentration, the evolution of both strain at failure and tensile strength showed a maximum around 5% NaOH concentration. The results also show that the strength and the strain at failure were almost proportional to the XRD CI (both with a coefficient of determination of 0.98). At the NaOH concentration of 5%, the increase in tensile strength was about 129%, while the elongation at failure was about 175%.

Table 1. Effect of NaOH Concentration on the Mechanical Properties and Crystallinity of the Raffia Fiber

NaOH % weight	Tensile strength (MPa)	Strain at failure (%)	Young's modulus (GPa)	Crystallinity index (%)	Crystallite size (nm)
0	527 ± 84	2.8 ± 0.7	26 ± 2	51	9.6
2.5	644 ± 139	4.8 ± 1.1	23 ± 1	56	11.2
5	1200 ± 150	7.7 ± 1.6	22 ± 2	68	13.5
10	956 ± 45	6.3 ± 0.8	18 ± 2	62	11.9

A density of 0.75 g/cm³ was reported for this fiber (Elenga *et al.* 2009), and the 5% treated fiber reached a specific strength value of 1600 MPa·cm³/g. This value is higher than that of E-glass and it is among highest of plant fibers in the Ashby's stress *versus* density chart. This level of treatment would be the best choice for material selection based on minimum weight design with $\sigma^{2/3}/\rho$ and $\sigma^{1/2}/\rho$, as discussed in a recent study (Monteiro *et al.* 2011).

The literature reports that the effect of alkaline treatment on plant fibers varies with the nature of the plant, the treatment time, temperature, and sodium content (Bledzki and Gassan 1999; Edeerozey *et al.* 2007; Nam *et al.* 2011). However, as reported in Table 2, at RT and for roughly the same NaOH concentrations considered here, similar evolutions of tensile strength and strain at failure were reported for coir (Nam *et al.* 2011), jute (Sahaet *et al.* 2010), kenaf (Edeerozey *et al.* 2007), Borassus fiber (Boopathi *et al.* 2012; Obi Reddy *et al.* 2013), and oil palm empty fruit bunches fibers (OPEFBF) (Norullzani *et al.* 2013). On the contrary, the Young's modulus of the treated raffia fiber decreased as that of the female date palm leaflet fiber (AlMaadeed *et al.* 2013), while that of the other fibers reported here increased as a result of the treatment. This change in mechanical properties is consistent with the reaction kinetics often described for NaOH-treated LCFs (Bledzki and Gassan 1999; Van de Weyenberg *et al.* 2006): for low concentrations or short immersion times, the solution partially dissolves the matrix of the fiber (hemicellulose, pectin, and lignin). This dissolution reduces the stiffness of the fiber and allows cellulose fibrils to expand during stretching (Bledzki and Gassan 1999).

Table 2. Effect of NaOH Treatment on Mechanical Properties of Some Lignocellulosic Fibers

Fiber	Soaking conditions at RT	Strength (MPa)		Young's modulus (GPa)		Strain at failure (%)		Ref.
		Raw	Treated	Raw	Treated	Raw	Treated	
Jute	4%, 24 h	370	554	-	-	1.3	2	Sahaet <i>et al.</i>
Kenaf	6%, 3 h	215	239	-	-			Edeerozey
Borassus fiber	5%, 0.5 h	118	175	-	-			Boopathi
Borassus fine f.	5%, 8 h	71	121	10.8	35.2	34.8	58.1	Reddy
OPEFBF	2%, 0.5 h	52	64	2.4	2.8	10	7	Izani <i>et al.</i>
Coir	5%, 72 h	140	238	2.8	5.9	29.5	34	Namet <i>et al.</i>
Coir	5%, 672 h	603	739			14.5	18	Gu
Raphia textilis	5%, 12 h	527	1200	26	18	2.8	6.3	This study

The extensibility of the fibers may explain the increase of strain at failure, while a better alignment of fibrils generates a greater tensile strength. However, treatment with higher concentrations of NaOH destroys the matrix and attacks cellulosic fibrils, thus leading to fiber weakening. The evolution of the Young's modulus with the treatment is more difficult to predict. Indeed, the dissolution of the cementing components (lignin and hemicellulose) decreases the fiber stiffness but the increase of the crystallinity and orientation could counterbalance this decrease.

Color

As shown in Table 3, the alkali treatments increased the yellowness and the redness (or reduced the blueness and the greenness, respectively), but reduced the lightness. While the decrease (about 13%) in lightness did not vary significantly with the NaOH concentration, the increases in yellowness and the redness presented a maximum around the concentration of 2.5% (about 92% and 283%, respectively). Khan and Ahmad (1996) reported that alkaline treatment reduced the lightness of jute fiber by 10 to 20%. This decrease was attributed to the removal of lignin.

Table 3. Variation of Color with NaOH Treatment

NaOH % weight	L^*	a^*	b^*	$\Delta E^*(D65)$	$\Delta E^*(A)$	$\Delta E^*(F2)$
0	71.6±0.8	1.14±0.3	24.7±2.0	0	0	0
2.5	62.4±1.4	4.4±0.5	47.3±3.6	24.6±1.4	24.6±1.5	27.0±1.4
5	62.7±1.3	3.8±0.4	46.1±3.6	23.4±1.4	23.2±1.3	25.7±1.3
10	60.6±1.3	3.2±0.2	43.3±3.5	21.7±1.3	21.3±1.4	23.8±1.3

Chlorophylls are responsible for the green color in vegetables, while carotenoids are responsible for the yellow to red-orange color of vegetables. Due to their conjugated double bonds, plant pigments easily react in the presence of light, oxygen, and bases (Schoefs 2005). In particular, chlorophylls are easily degraded in alkaline solutions (Minguez-Mosquera and Gandul-Rojas 1995). Therefore, the large chroma increase, or decrease of the greenness observed for 2.5% treated fiber, is probably linked to chlorophyll degradation. For more concentrated solutions, the color decrease should be due to reactions of all pigments with the alkaline solution.

CONCLUSIONS

The objective of this study was to examine the effect of low concentrations of NaOH solution treatments on the microstructure, structure, composition, thermal behavior, mechanical behavior, and color of the *Raffia textilis* fiber. The results can be summarized as follows:

1. With a treatment of up to 5% NaOH, the strength and the strain to failure increased by about 129 and 175%, respectively, while the Young's modulus decreased slightly. The fiber reached a specific tensile strength of 1600 MPa·cm³/g, which is higher than that of E-glass. After 10% NaOH solution treatment, both the strength and the strain decreased.

2. The alkali treatment strongly increased the yellowness and the redness but slightly reduced the lightness. The maximum increases of yellowness and redness occurred after 2.5% NaOH solution treatment and were about 92 and 283%, respectively. The decrease of lightness was about 13%.
3. The onset of thermal degradation of the raw fiber (256 °C) was higher than the average value of plant fibers (219 °C) reported by Yao *et al.* (2008). It increased with NaOH treatment, up to 5% NaOH (278 °C).
4. The NaOH treatment removed the fiber's alveoli, hemicellulose, lignin, and pectin, but increased its clearness and smoothness.
5. The FTIR crystallinity index (CI) related to cellulose I_β (719/894) did not vary significantly up to 5% NaOH, but decreased by about 60% for 10% NaOH solution. For 10% NaOH-treated fibers, the decrease of the CI, the broadening of crystalline bands, the increase of the peak at 668 cm⁻¹, and the absorbance ratio of the bands at 983-993 and 1165 cm⁻¹ suggest the beginning of the transformation of cellulose I into cellulose II.
6. Although all XRD peaks exhibited by the raw and treated fibers were the same and could be attributed to cellulose I_β, the change of the diffractogram shape of the 10% NaOH treated fiber was probably due to the swelling of crystallites. This is also an indication of the beginning of the transformation of cellulose I. Additionally, the 5% NaOH-treated fiber had the greatest XRD CI and crystallite size.

ACKNOWLEDGMENTS

Part of this work was conducted in the framework of the "Emerging Materials" project financially supported by *Institut Fédérative de Recherche, IFR Matériaux* at Université Paris 13, Sorbonne Paris Cité. R. G. Elenga is grateful to the MSE Department at Saint Denis Institute of Technology for making its experimental facilities available.

REFERENCES CITED

- Alawar, A., Hamed, A. M., and Al-Kaabi, K. (2009). "Characterization of treated date palm tree fiber as composite reinforcement," *Composites Part B: Engineering* 40(7), 601-606.
- AlMaadeed, M. A., Kahraman, R., Noorunnisa Khanam, P., and Al-Maadeed, S. (2013). "Characterization of untreated and treated male and female date palm leaves," *Materials & Design* 43, 526-531.
- Alsaed, T., Yousif, B. F., and Ku, H. (2013). "The potential of using date palm fibres as reinforcement for polymeric composites," *Materials & Design* 43, 177-184.
- Bansal, P., Hall, M. I., Realff, M. J., Lee, J. H., and Bommarius, A. S. (2010). "Multivariate statistical analysis of X-ray data from cellulose: A new method to determine degree of crystallinity and predict hydrolysis rates," *Bioresource Technology* 101(12), 4461-4471.
- Bledzki, A. K., and Gassan, J. (1999). "Composites reinforced with cellulose based fibres," *Progress in Polymer Science* 24(2), 221-274.

- Bociiek, S. M., and Welti, D. (1975). "The quantitative analysis of uronic acid polymers by infrared spectroscopy," *Carbohydrate Research* 42(2), 217-226.
- Boopathi, L., Sampath, P. S., and Mylsamy, K. (2012). "Investigation of physical, chemical and mechanical properties of raw and alkali treated Borassus fruit fiber," *Composites Part B: Engineering* 43(8), 3044-3052.
- Chapados, C. (1985). "Aggregation of chlorophylls in monolayers: VI. Infrared study of the CH stretching bands of chlorophyll a and of chlorophyll b in monolayers," *Biophysical Chemistry* 21(3-4), 227-242.
- D' Almeida, A. L. F. S., Barreto, D. W., Calado, V., and D' Almeida, J. R. M. (2008). "Thermal analysis of less common lignocellulose fibers," *Journal of Thermal Analysis and Calorimetry* 91(2), 405-408.
- Edeerozey, A. M. M., Akil, H. M., Azhar, A. B., and Ariffin, M. I. Z. (2007). "Chemical modification of kenaf fibers," *Materials Letters* 61(10), 2023-2025.
- Edem, D. O., Eka, O. U., and Ifon, E. T. (1984). "Chemical evaluation of the nutritive value of the raffia palm fruit (*Raphia hookeri*)," *Food Chemistry* 15(1), 9-17.
- Elenga, R. G., Dirras, G. F., Goma Maniongui, J., Djemia, P., and Biget, M. P. (2009). "On the microstructure and physical properties of untreated raffia textilis fiber," *Composites Part A: Applied Science and Manufacturing* 40(4), 418-422.
- Elenga, R. G., Dirras, G. F., Goma Maniongui, J., and Mabiala, B. (2011). "Thin-layer drying of raffia textilis fiber," *BioResources* 6(4), 4135-4144.
- Fink, H. P., Hofmann, D., and Philipp, B. (1995). "Some aspects of lateral chain order in cellulose from X-ray scattering," *Cellulose* 2(1), 51-70.
- George, J., Sreekala, M. S., and Thomas, S. (2001). "A review on interface modification and characterization of natural fiber reinforced plastic composites," *Polymer Engineering & Science* 41(9), 1471-1485.
- Hindeleh, A. M., and Johnson, D. J. (1980). "An empirical estimation of Scherrer parameters for the evaluation of true crystallite size in fibrous polymers," *Polymer* 21(8), 929-935.
- Jawaid, M., and Abdul Khalil, H. P. S. (2011). "Cellulosic/synthetic fibre reinforced polymer hybrid composites: A review," *Carbohydrate Polymers* 86(1), 1-18.
- Jiang, G., Huang, W., Wang, B., Zhang, Y., and Wang, H. (2012). "The changes of crystalline structure of cellulose during dissolution in 1-butyl-3-methylimidazolium chloride," *Cellulose* 19(3), 679-685.
- John, M. J., and Thomas, S. (2008). "Biofibres and biocomposites," *Carbohydrate Polymers* 71(3), 343-364.
- Khan, F., and Ahmad, S. R. (1996). "Chemical modification and spectroscopic analysis of jute fibre," *Polymer Degradation and Stability* 52(3), 335-340.
- Koh, L. P., Ghazoul, J., Butler, R. A., Laurance, W. F., Sodhi, N. S., Mateo-Vega, J., and Bradshaw, C. J. A. (2010). "Wash and spin cycle threats to tropical biodiversity," *Biotropica* 42(1), 67-71.
- Kondo, T., and Sawatari, C. (1996). "A Fourier transform infra-red spectroscopic analysis of the character of hydrogen bonds in amorphous cellulose," *Polymer* 37(3), 393-399.
- Kostic, M., Pejic, B., and Skundric, P. (2008). "Quality of chemically modified hemp fibers," *Bioresource Technology* 99(1), 94-99.
- Luangkiattikhun, P., Tangsathitkulchai, C., and Tangsathitkulchai, M. (2008). "Non-isothermal thermogravimetric analysis of oil-palm solid wastes," *Bioresource Technology* 99(5), 986-997.

- Minguez-Mosquera, M. I., and Gandul-Rojas, B. (1995). "High-performance liquid chromatographic study of alkaline treatment of chlorophyll," *Journal of Chromatography A*, 690(2), 161-176.
- Monteiro, S., Lopes, F. D., Barbosa, A., Bevitori, A., Silva, I. O., and Costa, L. (2011). "Natural lignocellulosic fibers as engineering materials: An overview," *Metallurgical and Materials Transactions A*, 42(10), 2963-2974.
- Nam, T. H., Ogihara, S., Tung, N. H., and Kobayashi, S. (2011). "Effect of alkali treatment on interfacial and mechanical properties of coir fiber reinforced poly(butylene succinate) biodegradable composites," *Composites Part B: Engineering* 42(6), 1648-1656.
- Norul Izani, M. A., Paridah, M. T., Anwar, U. M. K., Mohd Nor, M. Y., and H'ng, P. S. (2013). "Effects of fiber treatment on morphology, tensile and thermogravimetric analysis of oil palm empty fruit bunches fibers," *Composites Part B: Engineering* 45(1), 1251-1257.
- Obi Reddy, K., Uma Maheswari, C., Shukla, M., Song, J. I., and Varada Rajulu, A. (2013). "Tensile and structural characterization of alkali treated Borassus fruit fine fibers," *Composites Part B: Engineering* 44(1), 433-438.
- Oh, S. Y., Yoo, D. I., Shin, Y., and Seo, G. (2005). "FTIR analysis of cellulose treated with sodium hydroxide and carbon dioxide," *Carbohydrate Research* 340(3), 417-428.
- Saha, P., Manna, S., Chowdhury, S. R., Sen, R., Roy, D., and Adhikari, B. (2010). "Enhancement of tensile strength of lignocellulosic jute fibers by alkali-steam treatment," *Bioresource Technology* 101(9), 3182-3187.
- Satyanarayana, K. G., Guimaraes, J. L., and Wypych, F. (2007). "Studies on lignocellulosic fibers of Brazil. Part I: Source, production, morphology, properties and applications," *Composites Part A: Applied Science and Manufacturing* 38(7), 1694-1709.
- Schoefs, B. T. (2005). "Plant pigments: Properties, analysis, degradation," *Advances in Food and Nutrition Research*, Academic Press, 41-91.
- Sugiyama, J., Persson, J., and Chanzy, H. (1991). "Combined infrared and electron diffraction study of the polymorphism of native celluloses," *Macromolecules* 24(9), 2461-2466.
- Sun, R., Lawther, J. M., and Banks, W. B. (1996). "Effects of pretreatment temperature and alkali concentration on the composition of alkali-soluble lignins from wheat straw," *Journal of Applied Polymer Science* 62(9), 1473-1481.
- Tilman, D., Fargione, J., Wolff, B., D'Antonio, C., Dobson, A., Howarth, R., Schindler, D., Schlesinger, W. H., Simberloff, D., and Swackhamer, D. (2001). "Forecasting agriculturally driven global environmental change," *Science* 292(5515), 281-284.
- Van de Weyenberg, I., Chi Truong, T., Vangrimde, B., and Verpoest, I. (2006). "Improving the properties of UD flax fibre reinforced composites by applying an alkaline fibre treatment," *Composites Part A: Applied Science and Manufacturing* 37(9), 1368-1376.
- Yan, H., Hua, Z., Qian, G., Wang, M., Du, G., and Chen, J. (2009). "Analysis of the chemical composition of cotton seed coat by Fourier-transform infrared (FT-IR) microspectroscopy," *Cellulose* 16(6), 1099-1107.
- Yao, F., Wu, Q., Lei, Y., Guo, W., and Xu, Y. (2008). "Thermal decomposition kinetics of natural fibers: Activation energy with dynamic thermogravimetric analysis," *Polymer Degradation and Stability* 93(1), 90-98.

- Zafeiropoulos, N. E., Vickers, P. E., Baillie, C. A., and Watts, J. F. (2003). "An experimental investigation of modified and unmodified flax fibres with XPS, ToF-SIMS and ATR-FTIR," *Journal of Materials Science* 38(19), 3903-3914.
- Zugenmaier, P. (2001). "Conformation and packing of various crystalline cellulose fibers," *Progress in Polymer Science* 26(9), 1341-1417.
- Zuluaga, R., Putaux, J. L., Cruz, J., Vélez, J., Mondragon, I., and Gañán, P. (2009). "Cellulose microfibrils from banana rachis: Effect of alkaline treatments on structural and morphological features," *Carbohydrate Polymers* 76(1), 51-59.

Article submitted: January 18, 2013; Peer review completed: March 6, 2013; Revised version received and accepted: April 25, 2013; Published: April 29, 2013.